



# HHS Public Access

Author manuscript

*J Allergy Clin Immunol.* Author manuscript; available in PMC 2019 May 01.

Published in final edited form as:

*J Allergy Clin Immunol.* 2018 May ; 141(5): 1943–1947.e9. doi:10.1016/j.jaci.2018.01.027.

## Germline Gain-of-Function *MYD88* Mutation in a Child with Severe Arthritis

Keith A. Sikora, MD<sup>a</sup>, Joshua R. Bennett, BS<sup>a</sup>, Laurens Vyncke, MS<sup>b,c</sup>, Zuoming Deng, PhD<sup>d</sup>, Wanxia Li Tsai, MS<sup>d</sup>, Ewald Pauwels, PhD<sup>e</sup>, Gerlinde Layh-Schmitt, PhD<sup>a</sup>, April Brundidge, BSN<sup>f</sup>, Fatemeh Navid, PhD<sup>a</sup>, Kristien J. M. Zaal, PhD<sup>d</sup>, Eric Hanson, MD<sup>g</sup>, Massimo Gadina, PhD<sup>d</sup>, Louis M. Staudt, MD, PhD<sup>h</sup>, Thomas A. Griffin, MD, PhD<sup>i</sup>, Jan Tavernier, PhD<sup>b,c</sup>, Frank Peelman, PhD<sup>b,c</sup>, and Robert A. Colbert, MD, PhD<sup>a</sup>

<sup>a</sup>Pediatric Translational Research Branch, National Institute of Arthritis and Musculoskeletal and Skin Diseases, National Institutes of Health, Bethesda, MD

<sup>b</sup>VIB Medical Biotechnology Center, A. Baertsoenkaai 3, Ghent B-9000, Belgium

<sup>c</sup>Department of Biochemistry, Ghent University, Ghent B-9000, Belgium

<sup>d</sup>Office of Science and Technology, National Institute of Arthritis and Musculoskeletal and Skin Diseases, National Institutes of Health, Bethesda, MD

<sup>e</sup>Center for Molecular Modeling, Ghent University, Technologiepark 903, Zwijnaarde B-9052, Belgium

<sup>f</sup>Office of Clinical Director, National Institute of Arthritis and Musculoskeletal and Skin Diseases, National Institutes of Health, Bethesda, MD

<sup>g</sup>Autoimmunity Branch, National Institute of Arthritis and Musculoskeletal and Skin Diseases, National Institutes of Health, Bethesda, MD

<sup>h</sup>Lymphoid Malignancies Branch, Center for Cancer Research, National Cancer Institute, National Institutes of Health, Bethesda, MD

<sup>i</sup>Levine Children's Hospital at Carolinas Medical Center, Charlotte, NC

### Keywords

MyD88; arthritis; rash; neutrophil; chemokine; IL-6

---

Corresponding author: Keith A. Sikora, National Institutes of Health, Bldg 10 Rm 12S257, 10 Center Dr., Bethesda, MD 20892, Ph: +1 301-443-7961, F: +1 301-594-0917, keith.sikora@nih.gov.

The authors report no conflict of interests.

**Publisher's Disclaimer:** This is a PDF file of an unedited manuscript that has been accepted for publication. As a service to our customers we are providing this early version of the manuscript. The manuscript will undergo copyediting, typesetting, and review of the resulting proof before it is published in its final citable form. Please note that during the production process errors may be discovered which could affect the content, and all legal disclaimers that apply to the journal pertain.

## To the Editor

Myeloid differentiation primary response 88 gene (*MYD88*) encodes an essential adaptor protein connecting Toll-like receptor (TLR) and IL-1 receptor (IL-1R) signaling to activation of IL-1 receptor-associated kinases (IRAKs). Upon receptor stimulation, MyD88 oligomerizes causing recruitment and activation of IRAKs to form the myddosome (i.e. MyD88-signaling complex),<sup>1</sup> ultimately triggering activation of NF- $\kappa$ B and/or interferon regulatory factor 7.<sup>2</sup> Germline loss-of-function mutations in *MYD88* lead to immunodeficiency with recurrent pyogenic infections.<sup>3</sup> Somatic gain-of-function mutations contribute to certain B cell malignancies.<sup>4,5,6</sup> Here we report an individual with a *de novo* germline gain-of-function *MYD88* mutation, who has severe destructive arthritis and an intermittent rash.

The subject was a 14-year old Caucasian female with arthritis in small-to-medium sized joints since the age of 2 years leading to severe bone destruction and periarticular growth arrest (Fig 1, A). The asymmetric arthritis often followed minor trauma, initially resembling septic arthritis, but synovial fluid cultures were negative and antibiotics ineffective. Two synovial biopsies of chronic arthritis revealed a marked neutrophilic infiltrate (not shown), unlike the lymphocytic pattern seen in juvenile idiopathic arthritis (JIA). MRIs revealed substantial synovial, periarticular, and intramedullary bone inflammation (Fig 1, B). The arthritis was unresponsive to NSAIDs, methotrexate, and corticosteroids, while biologics had been declined. Intermittent rashes began around the onset of her arthritis and were erythematous and maculo-papular, generally lasting 1-2 weeks with spontaneous resolution (Fig 1, C). A recent skin biopsy from a dorsal hand lesion revealed interstitial granulomatous dermatitis. Whether this explains previous rashes is unclear. There was no history of unexplained fever, recurrent infection, or growth delay.

The subject's C-reactive protein has been intermittently elevated (but <7 mg/L; normal 0-4.99 mg/L), as has osteocalcin (113.8-201.6 ng/mL; normal 7.3-38.5 ng/mL), but with normal erythrocyte sedimentation rate, complete blood count, and serum immunoglobulins including IgG subsets. Lymphocyte subsets (CD3, CD4/CD3, CD8/CD3, CD19, and NK cells) were normal and no autoantibodies have been detected. For a summary of clinical findings, please see Table E1 in this article's Online Repository at [www.jacionline.org](http://www.jacionline.org).

The severe phenotype and inconsistencies with typical polyarticular JIA led us to pursue whole exome sequencing, which revealed a heterozygous missense mutation in *MYD88* (c.666T>G, p.Ser222Arg or S222R) in the patient, but not other family members, also confirmed by Sanger sequencing (see Fig E1, A, in this article's Online Repository at [www.jacionline.org](http://www.jacionline.org)). The mutation was present in ~50% of reads from patient whole blood, CD14+ monocytes, cultured dermal fibroblasts, and patient-derived B lymphoblastoid cells (EBV-LCL) supporting a strong likelihood that it is germline (see Fig E1, B).

Immunophenotyping revealed monocytes lacking CD16, which is known to shed during TLR activation,<sup>E1</sup> and identified a previously unreported CD123+CD11c+ dendritic cell population (Fig 1, D) that was negative for CD1c/BDCA-1, CD303/BDCA-2, CD141/BDCA-3, and the activated basophil marker CD203c (see Fig E2 in this article's Online

Repository at [www.jacionline.org](http://www.jacionline.org)). Additionally, CD19+CD20-CD27+CD38+ plasmablasts were absent and CD20+CD19+IgD-CD27+ memory B cells were decreased (Fig 1, D). Please see Table E1 for complete immunophenotyping data in this article's Online Repository at [www.jacionline.org](http://www.jacionline.org). There was a striking increase in Y705 STAT3 phosphorylation in unstimulated CD4+ and CD8+ T lymphocytes, a smaller increase in CD14+ monocytes, and a subpopulation of p-STAT3+ CD19+ B lymphocytes, as has been reported in gain-of-function *MYD88* mutation-positive malignancies.<sup>4,5</sup> STAT3 phosphorylation was similar to control cells after IL-6 stimulation, except for a population of highly phosphorylated CD8+ T lymphocytes in the patient (Fig 1, E). Neutrophil surface CD11b, CD66b, and CD62L expression was similar to controls (data not shown), possibly due to chronic homeostatic changes in rates of surface antigen shedding to production or cell death/clearance. Peripheral monocyte gene expression revealed an interferon-regulated signature (NanoString dataset available upon request, Fig 1, F), and *IL6* expression was also elevated, but not *TNF* (Fig 1, F). Whole blood production of TNF- $\alpha$  and IL-6 from unstimulated patient cells was higher than controls (Fig 1, G), while the differences did not persist after TLR-stimulation (data not shown).

Amino acid residue 222 is located on the surface of the MyD88 TIR domain, which is required for oligomerization and myddosome formation.<sup>1</sup> Oligomerization occurs via the BB-loop, the alpha E helix, and the C-terminus of the alpha helix C.<sup>7</sup> Using molecular dynamics modeling, we found that the S222R mutation is predicted to introduce a novel R222-E245 salt bridge that together with steric effects between R222 and F248 side chains, induces a significant tilt of the alpha C helix (see Fig E3, A, in this article's Online Repository at [www.jacionline.org](http://www.jacionline.org)). Similar to what is seen in the L265P activating mutation,<sup>7</sup> this shift of the CD loop may promote MyD88 TIR-TIR symmetrical interaction. Since the patient was heterozygous for S222R, we re-expressed equal amounts of wild-type (WT) and/or S222R MyD88 proteins with different epitope tags within the same MyD88-deficient (MyD88-KO) cell (see Fig E3, B). Unstimulated cells containing S222R MyD88 in conjunction with WT display 6-7-fold higher NF- $\kappa$ B activity compared to cells containing only WT or only S222R MyD88 (see Fig E3, C), consistent with previous findings.<sup>8</sup> Using a proximity ligation assay, S222R exhibited a 1.8-fold enhanced interaction with WT (using either tag combination) compared to interactions between two WT or two S222R-containing proteins (see Fig E3, D and E). These results demonstrate that the S222R mutation increases MyD88 interaction with WT MyD88, indicating that heterozygosity is sufficient for, and may actually maximize, MyD88 S222R gain-of-function effects.

We investigated MyD88 pathway activation in patient dermal fibroblasts, finding significantly elevated gene expression of several neutrophil-attracting chemokines (NanoString dataset available upon request). Elevations in *CXCL1*, *CXCL5*, and *CXCL8* were confirmed by qPCR (Fig 2, A), and at the protein level for *CXCL1* and IL-8 (see Fig E4, A, in this article's Online Repository at [www.jacionline.org](http://www.jacionline.org)). Patient fibroblast-conditioned media attracted healthy donor neutrophils to a greater extent than control-conditioned media (see Fig E4, B). MyD88 knockdown caused a significant reduction in *CXCL8* (Fig 2, B), which was not seen with knockdown of the upstream TIR-containing adaptor protein (TIRAP) (Fig 2, C). Downstream, the IRAK4 inhibitor AS2444697 caused a dose-dependent reduction in baseline *CXCL8*, with little effect in control cells (Fig 2, D).

Lastly, knockdown of NF- $\kappa$ B p65 subunit significantly reduced *CXCL8* to levels approaching control cells (Fig 2, E). Similar results were seen with *CXCL1* and *CXCL5* (not shown).

A20 (*TNFAIP3*), which negatively regulates the NF- $\kappa$ B pathway,<sup>E2</sup> was upregulated in patient-derived EBV-LCL (Fig 2, F) and fibroblasts (Fig 2, G). It has been previously reported that A20 upregulation in murine B lymphocytes containing MyD88 L265P limits NF- $\kappa$ B activation and proliferation.<sup>E3</sup> Knockdown of patient fibroblast A20 significantly increased *CXCL8* (10.1-fold), as well as *CXCL1* and *CXCL5* (not shown) and caused an emergence of *IL6* expression (Fig 2, H). These results suggest that A20 constrains – albeit incompletely - the increased activity of MyD88 S222R-regulated pathways producing pro-inflammatory mediators.

The S222R mutation has been reported in a single DLBCL cell line (SUDHL2),<sup>4</sup> where it leads to overproduction of IL-6.<sup>E4</sup> We confirmed and extended the SUDHL2 result to include IL-8 (see Fig E5, A, in this article's Online Repository at [www.jacionline.org](http://www.jacionline.org)), and demonstrate that patient-derived EBV-LCL with MyD88 S222R also overexpress IL-6/IL-8 at the mRNA and protein level in an IRAK4-dependent manner (see Fig E5, B). SUDHL2, like other *MYD88* mutation containing DLBCL cells, overexpress and hyper-phosphorylate STAT3 (Fig E5, C), which is believed to be due to autocrine IL-6.<sup>E4</sup> Similarly, patient-derived EBV-LCL exhibit increased p-STAT3 (Y705) (see Fig E5, D), although STAT3 expression is not increased. To directly assess the role of autocrine IL-6, we first treated DLBCL U2932 cells (expressing wild-type MyD88) with SUDHL2-conditioned media, which caused increased p-STAT3 that could be partially blocked by the IL-6 receptor antagonist tocilizumab (TCZ) (see Fig E5, E). Similarly, we exposed unrelated healthy control EBV-LCL to patient or mother EBV-LCL-condition media. Like SUDHL2 media, patient-conditioned media caused increased p-STAT3 in these cells, that could also be partially blocked with TCZ, demonstrating bioactive IL-6 secreted from patient B cells (see Fig E5, F). Both SUDHL2 and patient's EBV-LCL also overproduced IL-10 compared to control cells (data not shown), which could also be influencing Y705 p-STAT3 levels.

This is the first report of a germline gain-of-function mutation in *MYD88* (S222R) in a subject with destructive polyarthritis and rash. We show that S222R activates MyD88 confirming and extending previous observations,<sup>4,7,8</sup> and provide novel evidence for enhanced interaction with WT MyD88 as a plausible mechanism. Increased production of neutrophil-attracting chemokines and IL-6 are likely to contribute to the joint and skin phenotype, and the patient exhibited immunological perturbations consistent with increased MyD88 signaling, such as increased leukocyte p-STAT3, shedding of CD16, and increased whole blood secretion of IL-6 and TNF- $\alpha$ . Interestingly, our subject lacked evidence of lymphoproliferation. It is unlikely that S222R alone is sufficient to cause lymphoproliferation as the S222R-containing SUDHL2 cell line also harbors biallelic functional deletions of A20 and its re-expression arrests proliferation.<sup>E5</sup> Similarly, ectopic expression of S209R-MyD88 (the murine ortholog of S222R) in murine B cells does not induce proliferation.<sup>E3</sup> Further delineating the mechanism(s) by which MyD88 S222R leads to the clinical and immunological phenotype will require additional studies including animal modeling.

## Supplementary Material

Refer to Web version on PubMed Central for supplementary material.

## Acknowledgments

This research was supported by the Intramural Research Program of the National Institute of Arthritis and Musculoskeletal and Skin Diseases (Z01-AR041184), Pediatric Translational Research Branch, of the National Institutes of Health.

## References

1. Motshwene PG, Moncrieffe MC, Grossmann JG, Kao C, Ayaluru M, Sandercock AM, et al. An oligomeric signaling platform formed by the Toll-like receptor signal transducers MyD88 and IRAK-4. *J Biol Chem*. 2009; 284(37):25404–25411. [PubMed: 19592493]
2. Guven-Maiorov E, Keskin O, GURSOY A, VanWaes C, Chen Z, Tsai CJ, et al. The architecture of the TIR domain signalosome in the Toll-like receptor-4 signaling pathway. *Sci Rep*. 2015; 5:13128. [PubMed: 26293885]
3. von Bernuth H, Picard C, Jin Z, Pankla R, Xiao H, Ku CL, et al. Pyogenic bacterial infections in humans with MyD88 deficiency. *Science*. 2008; 321(5889):691–696. [PubMed: 18669862]
4. Ngo VN, Young RM, Schmitz R, Jhavar S, Xiao W, Lim KH, et al. Oncogenically active MYD88 mutations in human lymphoma. *Nature*. 2011; 470(7332):115–119. [PubMed: 21179087]
5. Puente XS, Pinyol M, Quesada V, Conde L, Ordóñez GR, Villamor N, et al. Whole-genome sequencing identifies recurrent mutations in chronic lymphocytic leukaemia. *Nature*. 2011; 475(7354):101–105. [PubMed: 21642962]
6. Treon SP, Xu L, Yang G, Zhou Y, Liu X, Cao Y, et al. MYD88 L265P somatic mutation in Waldenström's macroglobulinemia. *N Engl J Med*. 2012; 367(9):826–833. [PubMed: 22931316]
7. Vyncke L, Bovijn C, Pauwels E, Van Acker T, Ruysinck E, Burg E, et al. Reconstructing the TIR Side of the Myddosome: a Paradigm for TIR-TIR Interactions. *Structure*. 2016; 24(3):437–447. [PubMed: 26876098]
8. Avbelj M, Wolz OO, Fekonja O, Ben ina M, Repi M, Mavri J, et al. Activation of lymphoma-associated MyD88 mutations via allosteric-induced TIR-domain oligomerization. *Blood*. 2014; 124(26):3896–3904. [PubMed: 25359991]

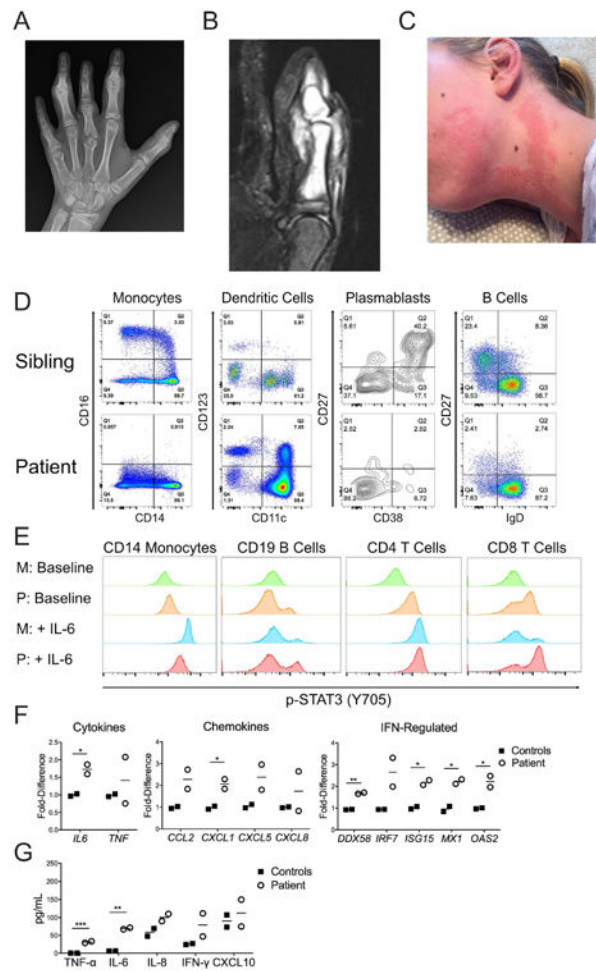


**Fig 1.** Clinical and immunological phenotype of patient with germline MyD88 S222R mutation. **A**, Left-hand radiograph. **B**, STIR MRI of left thumb. **C**, Appearance of recurrent rash. **D**, Representative immunophenotyping of monocytes, dendritic cells, plasmablasts, and B cells. Similar results were obtained 3 times over a span of 27 months, with sibling, mother, and an unrelated individual as controls. **E**, Representative histograms of baseline and IL-6 induced (50 ng/mL for 20 minutes) phosphorylation of STAT3 (p-STAT3, Y705) in patient (P) and mother (M) peripheral mononuclear cells by flow cytometry. Similar results were obtained twice, 6 months apart, with mother and unaffected sibling as controls. **F**, Baseline peripheral monocyte gene expression determined by qPCR. **G**, Cytokine secretion from 22 hour whole blood cultured without stimulation. For **F** and **G**, similar results were obtained twice, 1 year apart, using mother and unrelated healthy subject as controls. Lines represent the means. \*,  $p < 0.05$ ; \*\*,  $p < 0.01$ ; \*\*\*,  $p < 0.001$ .

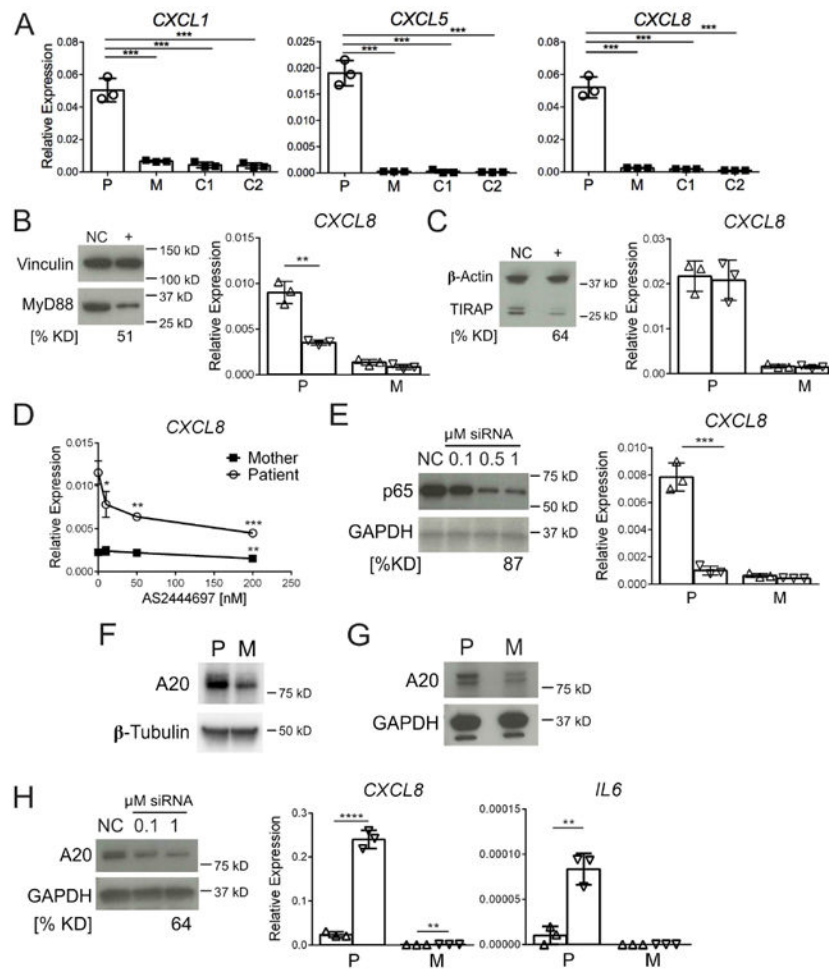


**Fig 2.** Enhanced neutrophil-attracting chemokine expression. **A**, Chemokine gene expression in dermal fibroblasts from patient (P), mother (M), and 2 unrelated healthy controls (C1 and C2). **B**, Effect of MyD88 knockdown on *CXCL8* gene expression. **C**, Effect of TIRAP knockdown on *CXCL8* gene expression. **D**, Effect of IRAK4 inhibitor (AS2444697) on *CXCL8* gene expression. Asterisks represent p-values comparing AS2444697 concentrations vs. baseline (0 nM) for each subject. **E**, Effect of NF- $\kappa$ B p65 knockdown on *CXCL8* gene expression. **F**, Baseline A20 protein expression in EBV-LCLs from patient (P) and mother (M). **G**, Baseline A20 protein expression in fibroblasts. **H**, A20 knockdown immunoblot in patient fibroblasts and resultant *CXCL8* and *IL6* gene expression. For knockdown blots, NC, negative control siRNA; (+), specific target knockdown; % KD, percent decrease from NC siRNA protein expression. Vinculin,  $\beta$ -Actin, GAPDH and  $\beta$ -Tubulin used as blot loading controls. For knockdown graphs, ( ) negative control siRNA and (∇) specific target siRNA. For all graphs, each data point represents the median of 3 replicates, with results from 3 independent experiments (n=3) shown. Error bars represent  $\pm$  SD. \*, p<0.05; \*\*, p<0.01; \*\*\*, p<0.001; \*\*\*\*, p<0.0001.